Supplementary Information to

Evidence of Electronic Phase Separation in the Strongly Correlated Semiconductor YbB_{12}"

A. Azarevich[1], N. Bolotina[2,1], O. Khrykina[2], A. Bogach[1], E. Zhukova[3], B. Gorshunov[3],

A. Melentev[3], Z.Bedran[3], A. Alyabyeva[3], M. Belyanchikov[3],

V. Voronov[1], N. Yu. Shitsevalova[4], V. B. Filipov[4], N. Sluchanko[1]

[1]Prokhorov General Physics Institute of the Russian Academy of Sciences, Vavilov str. 38, Moscow 119991, Russia

[2]Shubnikov Institute of Crystallography, Federal Scientific Research Centre 'Crystallography and Photonics' of Russian Academy of Sciences, 59 Leninskiy prospect, Moscow, 119333, Russia

[3]Center for Photonics and 2D Materials, Moscow Institute of Physics and Technology (National Research University), 141700 Dolgoprudny, Moscow Region, Russia

[4]Institute for Problems of Materials Science, NASU, Krzhizhanovsky str., 3, 03142 Kyiv, Ukraine

1. Terahertz-infrared measurements.

At terahertz frequencies (ν≈10-90 cm^{-1}), polarized spectra of the AC conductivity $\sigma(\nu)$ and of real $\varepsilon'(\nu)$ and imaginary $\varepsilon''(\nu)$ parts of dielectric permittivity were obtained with the time-domain spectrometer TeraView TPS 3000 by measuring the complex transmissivity of a thin (≈0.02 mm) plane-parallel sample of about 5 mm in diameter. For infrared measurements, a disk ~5 mm in diameter was used with plane-parallel (within ±1 μm) polished surfaces with indexes of {111} family. At infrared frequencies (ν=40-1000 cm^{-1}), polarized infrared reflectivity spectra $R(\nu)$ were measured using Vertex 80V Fourier-transform spectrometer with the gold films deposited on a glass substrate used as reference mirrors. Both samples were etched in the boiling HNO_3+H_2O solution to remove the surface layer with possible structural distortions. To get the terahertz-infrared spectra of AC conductivity and dielectric permittivity of the crystal we performed a Kramers-Kronig analysis of the merged terahertz-infrared reflectivity spectra, with the low-frequency Hagen-Rubens extrapolation according to the measured DC conductivity; for the high frequency extrapolation we utilized optical data from [S1]. Terahertz reflectivity was calculated using standard Fresnel equations basing on the measured conductivity and permittivity data. Low-temperature measurements down to T=3 K were performed using commercial cold finger (infrared experiments) and home-made helium-flow (terahertz experiments) cryostats.

2. XRD data analysis in YbB_{12}.

The measured values of the amplitudes of the structural factors $|F_{obs}|$ were averaged in the Laue class $m\bar{3}m$, and the crystal structure of YbB_{12} was refined in the symmetry group $Fm\bar{3}m$ at T = 107 K and 293 K [S2]. The data below are taken from [S2] to characterize the quality of the experiment and the results of refinement of the structural model.

T (K) (nominal)	100	293
T (K) (real)	107	293
Crystal system, space group	Cubic, Fm3m	Cubic, Fm3m
a (Å)	7.4600 (2)	7.4629 (1)
No. of measured, independent and		
observed [I > 3σ(I)] reflections	10 668, 267, 267	10 690, 267, 267
Rint	0.038	0.050
(sin θ/λ)max ($Å^{-1}$)	1.354	1.353
R[F^2 > 2σ(F^2)], wR(F^2), S	0.010, 0.014, 1.06	0.016, 0.023,1.01
No. of reflections	267	267
No. of parameters	7	7
Δρmax, Δρmin (e $Å^{-3}$)	1.24, -1.79	2.56, -0.81

An independent atomic set consists of two atoms. The Yb atom is fixed in position 4a (0,0,0). The boron atom is in a special position 48*i* (1/2, *y*, *y*). All atoms are provided with anisotropic thermal parameters (atomic displacement parameters, ADP in modern nomenclature). So, refined structural parameters are limited by one coordinate (*y*) of the boron atom and ADPs of B and Yb atoms.

Fine details of atomic structure can be derived from residual electron density (ED) distribution taking difference Fourier maps into consideration. Fourier synthesis of ED is a computational procedure, which starts with a set of both experimental and previously calculated parameters. Computational formula can be written in general terms as follows:

$$\sigma(\mathbf{r}) = (1/V)\Sigma_{\mathbf{H}} A(\mathbf{H})\exp[i\varphi(\mathbf{H})] \exp(-2\pi i \mathbf{Hr}) \qquad (1)$$

Here σ is either electron density *g* or residual (difference) electron density Δ*g* for a 'regular' or difference Fourier synthesis, respectively; *V* is a unit-cell volume; $\mathbf{H} = \Sigma h_i \mathbf{a}^*_i$ is a Bragg vector;

$A(\mathbf{H})$ is either $|F_{obs}(\mathbf{H})|$ or $||F_{obs}(\mathbf{H})| - |F_{calc}(\mathbf{H})||$ in case of 'regular' or difference Fourier synthesis, respectively; $\varphi(\mathbf{H})$ can be calculated if atomic coordinates are known. Values $|F_{calc}|$ are calculated from the refined structure model.

The formula (1) does not contain any information on the crystal symmetry. To align the synthesis results with the symmetry of the structural model, a computational program supports ED calculations in a symmetry-independent part of the unit cell using symmetry-averaged $|F|_{obs}$ instead of individual values. The result is then expanded on the whole cell by the group-symmetry operators.

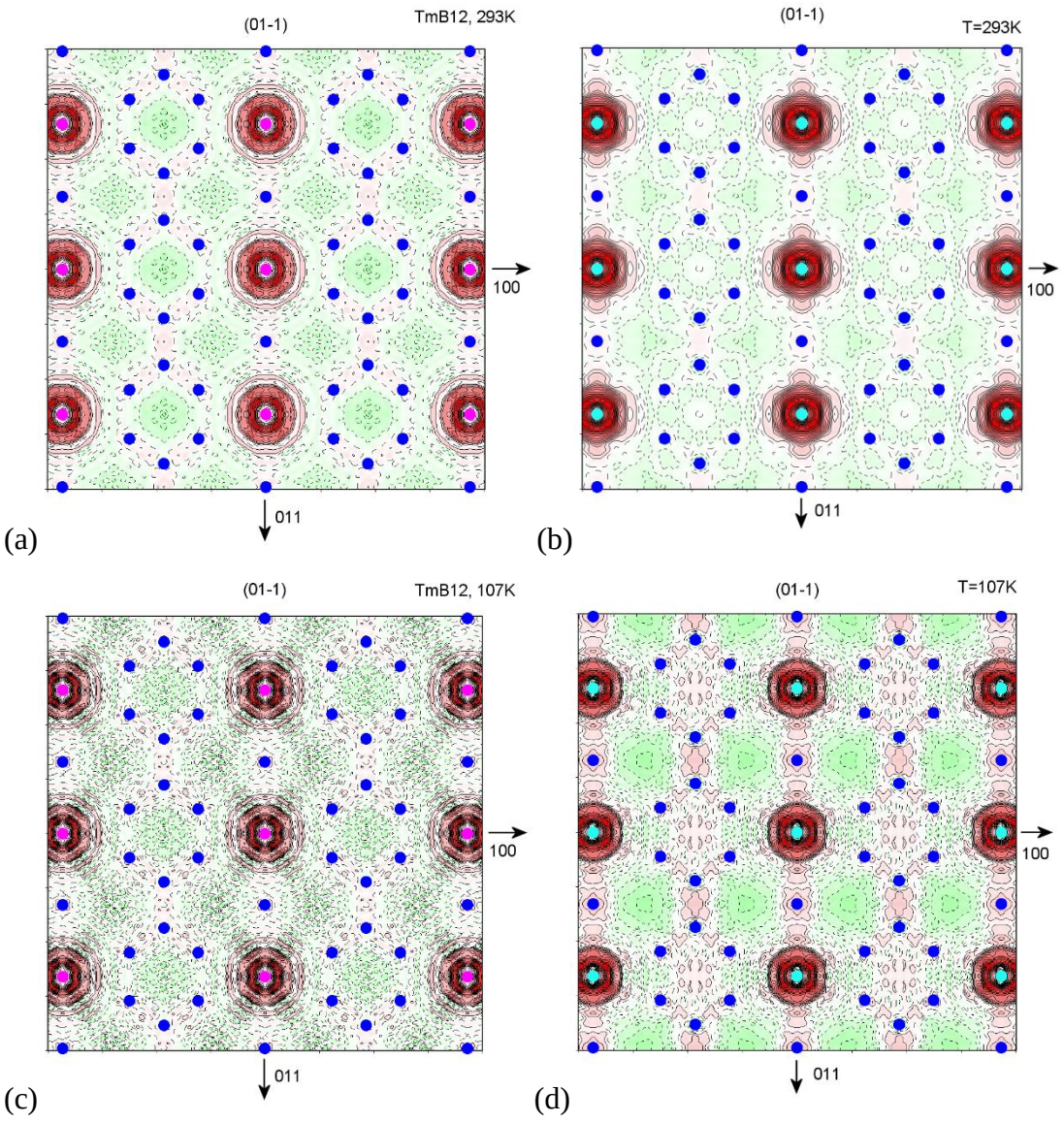

Fig.S1. Difference Fourier map of electron density Δg in TmB_{12} (a, c) and YbB_{12} (b, d) crystals studied at temperatures 107 K and 293 K. The (01-1) plane of 3D map is presented. The blue circles indicate the boron positions in the plane or near the plane; the light blue and pink circles mark the Yb and Tm positions, respectively. Shades of green and red indicate areas on the map with negative and positive values of Δg, respectively. Contour intervals are 0.2 e/Å^3.

3. Hall effect measurements.

Hall resistivity on $YbB_{12}$was detected in two ways:

(a) The traditional technique for the Hall effect was applied, where we calculate the value of Hall coefficient as $R_H = \rho_H/H = [(V_H(+H) - V_H(-H))/(2I)]\cdot d/H$, where I is the measuring current through the sample, d is the thickness of the sample (i.e., the sample size along the normal **n** to lateral surface), and $V_H(+/-H)$ are the voltages measured from Hall probes in two opposite orientations of the external magnetic field $\mathbf{H} \perp \mathbf{I}$, and

(b) The angular dependences of Hall resistivity are obtained using a measuring cell of an original design, which provides the rotation of the vector **H** located in the plane perpendicular to the fixed current direction **I** || [110] with a minimum step $\Delta\varphi = 0.4°$ (see the schematic view on the inset in fig. 1c in the manuscript). The measurements were carried out in a wide temperature range 1.9 - 300 K in magnetic fields up to 80 kOe, the angle $\varphi = \mathbf{n}\hat{}\mathbf{H}$ between the direction of the normal **n** to the lateral surface of sample and external magnetic field **H** varied in the range $\varphi = 0 - 360°$. The measuring setup was equipped with a stepper motor with automatic control of stepwise rotation of the sample. High accuracy of stabilization of temperature ($\Delta T \approx 0.002$K in the range 1.9 - 7K) and magnetic field ($\Delta H \approx 2$ Oe) was ensured, respectively, by Cryotel TC 1.5/300 temperature controller and Cryotel SMPS 100 superconducting magnet power supply in combination with CERNOX 1050 thermometer and n-InSb Hall sensors.

The magnetization measurements of YbB_{12} were carried out on the MPMS-5 installation (Quantum Design). Small paramagnetic response ($\sim 4\cdot 10^{-3}$ emu/(mole·Oe) at T<15 K (Fig. S2) allows estimating the upper limit of the demagnetizing factor correction to the magnetic field strength as 0.1%.

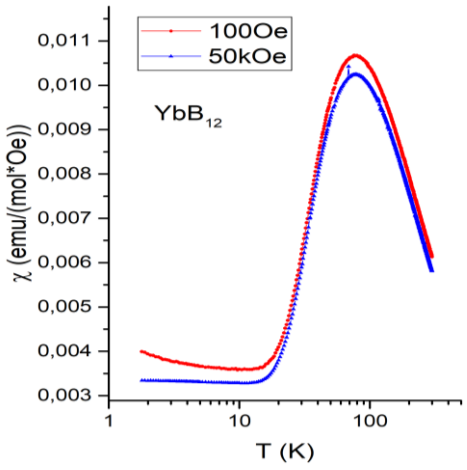

Fig.S2. Magnetic susceptibility $\chi(T, H_0)$ of YbB12 at H_0= 100 Oe and 50 kOe.

4. The gap values detected for YbB_{12} and $Tm_{1-x}Yb_xB_{12}$ in previous experiments.

The evaluated indirect gap $E_g/k_B \approx 216$ K (Fig.1b in the paper) appears to be close to the estimate of the gap value found for YbB_{12} in the measurements of the Hall effect and resistivity ($E_g/k_B \approx$ 180 and 134 K, respectively [S3]), NMR on the Yb ions and specific heat ($E_g/k_B \approx$ 170 K, [S4, S5], correspondingly) and Seebeck coefficient (~160 K, [S6]). This is also comparable to the spin gap value ≈ 12 meV found in the neutron scattering [S7,S8] and ESR [S9] experiments. The smaller activation energy (the intra-gap excitations) previously detected from transport measurements varies from E_a/k_B~25-28 K [S3, S10] to 40 K [S11]. To the best of our knowledge, the anisotropy of E_a/k_B has not yet been discussed for YbB_{12} crystals.

[S1]. B. Gorshunov, P. Haas, O. Ushakov, M. Dressel, F. Iga, "Dynamics of the coherent ground state in intermediate-valent YbB_{12}"; *Phys. Rev. B* **73**, 045207 (2006).

[S2]. N. Bolotina, O. Khrykina, A. Azarevich, S. Gavrilkin, N. Sluchanko, "Fine details of crystal structure and atomic vibrations in YbB_{12} with a metal–insulator transition", *Acta Crystallogr. B*, **76**, 1117 (2020).

[S3].F. Iga, N. Shimizu, and T. Takabatake, J. Magn. Magn.Mat. **177–181**, 337 (1998).

[S4]. K. Ikushima, Y. Kato, M. Takigawa, et al., Physica B**281–282**, 274 (2000).

[S5]. F. Iga, S. Hiura, J. Klijn, et al., Physica B **259–261**, 312(1999).

[S6]. N.E. Sluchanko et al., *JETP Lett., 89, 256–259 (2009)*

[S7]. J. M. Mignot, P. A. Alekseev, K. S. Nemkovski, et al., Phys. Rev. Lett. **94**, 247204 (2005).

[S8]. K. S. Nemkovski, J. M. Mignot, P. A. Alekseev, et al., Phys. Rev. Lett. **99**, 137204 (2007).

[S9]. T. S. Al'tshuler, A. E. Al'tshuler, and M. S. Bresler, Zh. Eksp. Teor. Fiz. **120**, 127 (2001) [JETP **93**, 111 (2001)].

[S10]. M. Kasaya, F. Iga, M. Takigawa, T. Kasuya, J. Magn. Magn. Mat. **47-48**, 429 (1985).

[S11]. S. Kayama, S. Tanaka, A. Miyake, T. Kagayama, K. Shimizu, and F. Iga, "Pressure induced insulator-to-metal transition at 170 GPa of Kondo semiconductor YbB_{12}"; *Proceedings of the International Conference on Strongly Correlated Electron Systems (SCES 2013), JPS Conf. Proc.* **3**, 012024 (2014).